

Dynamical properties of epitaxial CaF_2 films deposited on an Si(001) substrate studied by Brillouin spectroscopy

This article has been downloaded from IOPscience. Please scroll down to see the full text article.

1994 J. Phys.: Condens. Matter 6 10713

(<http://iopscience.iop.org/0953-8984/6/49/014>)

View [the table of contents for this issue](#), or go to the [journal homepage](#) for more

Download details:

IP Address: 171.66.16.179

The article was downloaded on 13/05/2010 at 11:29

Please note that [terms and conditions apply](#).

Dynamical properties of epitaxial CaF_2 films deposited on an $\text{Si}(001)$ substrate studied by Brillouin spectroscopy

V V Aleksandrov†, V M Saphonov†, N L Yakovlev‡ and V R Velasco§

† Chair for Crystallophysics, Physics Department, Moscow State University, Moscow 117234, Russia

‡ A F Ioffe Physico Technical Institute of Russian Academy of Science, St Petersburg 194021, Russia

§ Instituto de Ciencia de Materiales, CSIC, Serrano 123, E-28006, Madrid, Spain

Received 22 July 1994

Abstract. Using Brillouin spectroscopy we have studied the dynamical properties of epitaxial CaF_2 films, with thicknesses in the range $h = 61\text{--}300\text{ nm}$, grown on $\text{Si}(001)$ substrates. Theoretical calculations for the velocity values, based on a simple elastic continuum model, give results that agree quite well with experiment. A correlation between the dynamical properties of $\text{CaF}_2/\text{Si}(001)$ systems and their structure is found and discussed.

1. Introduction

As was pointed out in [1], the presence of an overlayer on top of the surface of a solid medium considerably modifies the spectrum of free surface excitations. For a certain relation between the elastic properties of the constituent materials (i.e. when the velocity of the transverse bulk mode of the layer material is lower than that of the substrate), the Rayleigh mode velocity decreases when the film thickness increases, and new normal modes of the structure (of Sezawa or Love type) appear.

The description of the modification of the surface excitation spectrum is further complicated if one takes into account the anisotropy of the elastic properties of the materials involved in the layered structure. In general, the Rayleigh mode loses its pure sagittal character, and becomes what is commonly termed a generalized surface wave (GSW). In addition, pseudo-surface modes (PSM) can also be present. These modes are leaky and radiate their energy into the bulk as they propagate along the surface. However, in many known cases the leakage is small and the PSM influences significantly the excitation spectrum of the whole layered system [2].

The anisotropic substances are usually characterized by their elastic anisotropy ratio, which may be ≥ 1 . Anisotropy is important, for example, in structures based on CaF_2 and Si, which have wide potential applications in microelectronics [3]. Both CaF_2 and Si have cubic symmetry, but a different type of elastic anisotropy described by the ratio $\mu = 2C_{44}/(C_{11} - C_{12})$ which is $\mu = 1.57 > 1$ (Si), and $\mu = 0.53 < 1$ (CaF_2) [4, 5].

The latter should give different laws of azimuthal dispersion of the GSW velocity and different behaviour of the PSM branch in the materials involved.

The problem of the propagation of surface acoustic modes for certain high-symmetry orientations presented by $\text{CaF}_2/\text{Si}(110)$, $\text{CaF}_2/\text{Si}(111)$ layered systems, and gradual transformations of the modes with the variation of film thickness, were described in [5–8].

The aim of the work described in this paper is to investigate the propagation of surface acoustic excitations in thin CaF_2 layers deposited on an $\text{Si}(001)$ substrate, and to discuss some features of the dynamical properties of these systems associated with the structure of the layer not present in other situations studied previously.

In section 2 we discuss the (001) surface excitations in Si and CaF_2 . In section 3 we describe the materials, experimental techniques and methods used in our study. Section 4 includes the experimental results and a discussion, while an explanation of the correlation between the dynamical properties of $\text{CaF}_2/\text{Si}(001)$ systems and their structure is presented in section 5. Conclusions are drawn in section 6.

2. (001) plane surface excitations in Si and CaF_2

The angular dispersion of the GSW velocity on the basal plane of bulk Si (substrate material), and CaF_2 (layer material) is presented in figure 1.

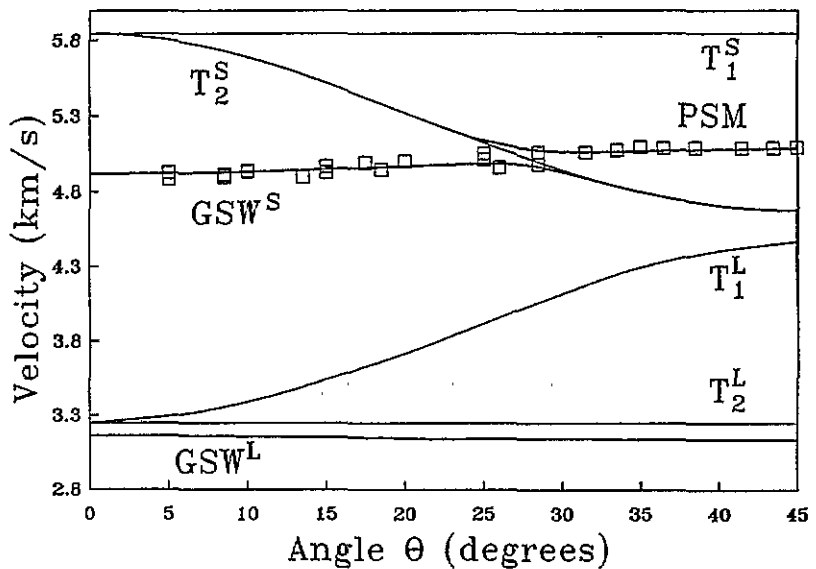


Figure 1. Si and CaF_2 angular dependence of surface and bulk (transverse) acoustic velocity values on θ in the (001) plane. Here θ is the angle between the [100] crystal axis and the propagation direction. The superscripts S and L refer to the substrate (Si) and layer (CaF_2) respectively. Thick full curves: calculated GSW^S and PSM. Thin full curves: calculated T_1^S and T_2^S . Squares: Brillouin spectroscopy data [15]. The curves were calculated using the stiffness coefficients of [5]. T_1 and T_2 indicate the transverse modes of each material.

In the case of Si at $\theta = 0^\circ$ the GSW surface-displacement ellipse is parallel to the sagittal plane. This is also true for the displacements of GSW in CaF_2 in this propagation direction. Here θ is the azimuthal angle between the [100] crystal axis and the direction of propagation. As soon as one leaves the [100] direction the anisotropic nature of the constituent materials manifests itself in various features of the surface acoustic excitation on the (001) plane [4].

For Si the displacement ellipse shifts gradually out of the sagittal plane, being perpendicular to it for [110] ($\theta = 45^\circ$), and its velocity becomes minimal. Additionally,

the shear vertical component of the displacements decreases, following the motion of the ellipse plane, and is zero for the [110] diagonal. In consequence, the GSW then degenerates into a shear horizontal bulk mode T_2^s satisfying free boundary conditions at $\theta = 45^\circ$.

Starting at $\theta = 22^\circ$ the PSM branch emerges, and at $\theta = 45^\circ$ the PSM transforms into a purely sagittal true surface mode.

As for the layer material, the GSW velocity is nearly independent of θ and its displacement ellipse lies in the sagittal plane for $\theta = 0^\circ$ and 45° , deviating from the sagittal plane at intermediate θ values.

Obviously, the acoustical properties of the (001) surface of the substrate and film material differ strongly from each other. For the substrate one predicts the presence of the PSM in a certain propagation sector including [110], and at the same time no dependence of the GSW velocity on the azimuth for the material of the film is expected.

The opposite properties of the constituents should affect the propagation behaviour of the GSW and higher-order modes in the $\text{CaF}_2/\text{Si}(001)$ system.

To obtain a complete description of the dynamical properties of the $\text{CaF}_2/\text{Si}(001)$ system one should analyse the surface excitation propagation for films of various thicknesses, h , and for different propagation directions in the (001) plane.

3. Materials, instruments and methods

The CaF_2 films were grown by molecular beam epitaxy in a research chamber [9]. Silicon wafers were chemically etched and thermally cleaned at 1250°C in the chamber. The Si substrate was kept at 600°C during the growth, which is an optimum temperature for the growth of epitaxial CaF_2 on $\text{Si}(001)$ [10, 11]. The deposition rate was $3\text{--}5\text{ nm min}^{-1}$. Later, the films were flattened *in situ* at 900°C . The structure of the layer was monitored using high-energy electron diffraction during the growth and the flattening, finally showing rather good crystalline quality.

Specimens with film thickness $h = 61, 80, 100, 150, 151, 170$ and 300 nm were investigated. The thickness was measured using both ellipsometry (for details, see [12]) and interferometric methods.

The dynamical properties of $\text{CaF}_2/\text{Si}(001)$ epitaxial systems were studied by Brillouin spectroscopy [13]. The light source was a single-frequency Ar^+ ion laser at $\lambda = 514.5\text{ nm}$ and of power $50\text{--}100\text{ mW}$ (Spectra-Physics 165-03). Backscattering was observed and analysed with a five-pass piezo-scanned Fabry-Perot interferometer (Burleigh). The free spectral range of the interferometer was 42.8 GHz and the finesse exceeded 60. The electric vector E lay in the plane of incidence in all experiments (p-p+s scattering configuration). The angle of incidence, α , was varied from 50° to 70° . Observations were conducted at room temperature.

The surface Green function matching method was used for the calculation of the surface excitation spectra, and for the velocity determination [14]. The simple elastic continuum model of [1] was used to describe the dynamical properties of the constituent materials forming the system under investigation.

4. Experimental results and discussion

The squares in figure 1 are the measured velocity values on the (001) free surface of Si [15]. These values were calculated from the frequency shifts δf of corresponding satellites of

light scattering spectra, $V = \delta f \lambda / 2 \sin(\alpha)$, where λ is the wavelength of the incident laser beam.

CaF_2 is characterized by strong elasto-optic coupling that masks the light scattered from surface excitations in the case of bulk samples. However, the measurements conducted with an opaque PbS cubic crystal of (001) cut having a similar elastic anisotropy parameter ($\mu = 0.507$) showed good coincidence between calculated GSW velocity values and those determined from δf for all non-equivalent directions in the plane [16].

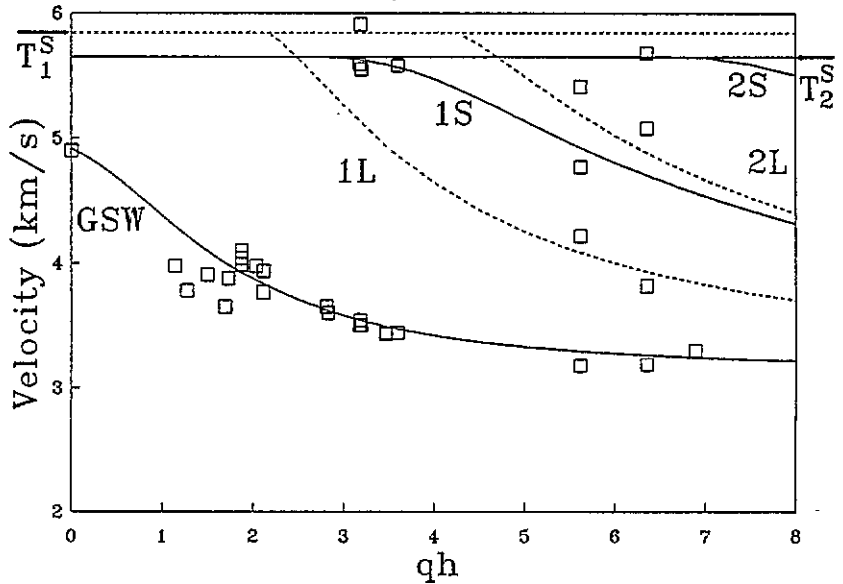


Figure 2. Velocities of the normal surface modes of $\text{CaF}_2/\text{Si}(001)$ structures, for the [100] propagation direction ($\theta = 0^\circ$), as a function of the normalized thickness qh . Experimental values are shown by squares. Sagittal modes (GSW, 1S, 2S) are represented by full curves, while the shear horizontal (Love) modes (1L, 2L) are shown by broken curves. The full horizontal line is the threshold for the Sezawa modes, while the broken horizontal line is the corresponding threshold for the shear horizontal ones. Note that L and S here do not have the same meaning as in figure 1.

Figure 2 gives the measured velocities of the normal surface modes of all the structures investigated for the [100] propagation direction; qh is the normalized thickness, and q is the surface wavevector.

With the variation of qh from 0 to 8, the GSW velocity decreases from 4.92 to 3.23 km s^{-1} , approaching its limit given by the GSW velocity of the layer material. At certain qh the calculations bear out the appearance of the normal modes of the layer for $qh \sim 2.1$ (first Love mode), $qh \sim 3.0$ (first Sezawa mode), $qh \sim 4.4$ (second Love mode), $qh \sim 6.4$ (second Sezawa mode). The sagittal modes (GSW, Sezawa) are shown by full curves, and the Love modes are shown by broken curves.

The velocity of the bulk mode of the substrate material is shown by an arrow on the vertical axis. The threshold limit for shear horizontal surface excitations coincides with it, whereas that of the sagittal one is lower, as may be in the case of elastically anisotropic media [17].

Figure 2 shows that the experimental values agree with the calculated GSW curve in the whole span of $qh = 0-8$. Reasonable correlation between measured and calculated values is also observed for the first Love mode ($qh \sim 6$), the first Sezawa mode ($qh \sim 3-7$), the second Love mode ($qh \sim 6$), and the second Sezawa mode ($qh > 6$).

One should remark that in the $p - p + s$ configuration the scattering of light by the surface of opaque media is mainly from ripples that are sensitive to the shear vertical surface excitations (see, for example, [18]). However, with increase in the CaF₂ film thickness the counterpart of pre-surface elasto-optic coupling associated with the longitudinal and shear-horizontal surface excitations becomes significant [19, 20]. Thus at a certain film thickness comparable with the probing light wavelength, $h \geq 300$ nm ($qh \geq 6$), the spectra of light scattered by CaF₂/Si(001) heterostructures contain the lines of pure Love (shear horizontal) modes in addition to the 'traditional' peaks corresponding to the sagittal normal modes.

At $qh = 1-2$ the experimental values of the GSW are 10% lower than the calculated values. In all cases presented here the experimental errors are of the order of 1-2% for GSW velocity values, and 3-4% for all the others.

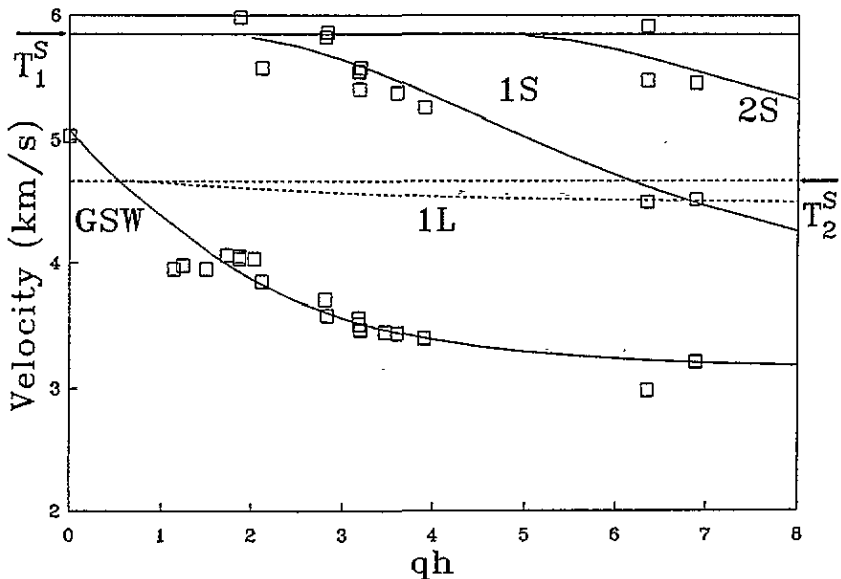


Figure 3. Velocities of the normal surface modes of CaF₂/Si(001) structures, for the [110] propagation direction ($\theta = 45^\circ$), as a function of the normalized thickness qh . Same conventions as in figure 2.

The results for the velocity of the surface normal modes propagating along [110] ($\theta = 45^\circ$) are presented in figure 3. Here, as in the previous case, the normal modes have a pure, i.e. sagittal, or shear-horizontal character.

Let us recall that at $\theta = 45^\circ$ the PSM transforms into the normal mode, having purely sagittal displacements, whereas the GSW becomes degenerate with the bulk shear-horizontal mode satisfying free boundary conditions, see figure 1. In consequence, the sagittal threshold keeps its velocity value close to that of T_1^s , while the shear horizontal bulk limit has the lower value.

As one leaves $qh = 0$ (figure 3) the GSW velocity decreases from 5.08-3.19 km s⁻¹ approaching the GSW velocity value of the layer material for $qh > 6$. Starting from $qh = 2.0$

and $qh = 4.8$ the local sagittal modes of the film appear (first and second Sezawa modes, respectively). Independently, the first Love mode starts in the vicinity of $qh = 1$.

Good agreement between measured and calculated values is obtained for sagittal polarized modes (GSW, first and second Sezawa modes). For $qh > 6$ the Brillouin lines corresponding to the first Love mode were detected, having δf (velocities) reasonably estimated by the theoretical values. The lowering of the experimental values of the GSW mode similar to that detected for $\theta = 0^\circ$ is also observed.

For the intermediate propagation directions, $0^\circ < \theta < 45^\circ$, the situation is more complicated because of the mixed character of the normal modes of the materials involved, see figure 1. As an illustrative case, we shall discuss the $\theta = 30^\circ$ direction, which is represented in figure 4.

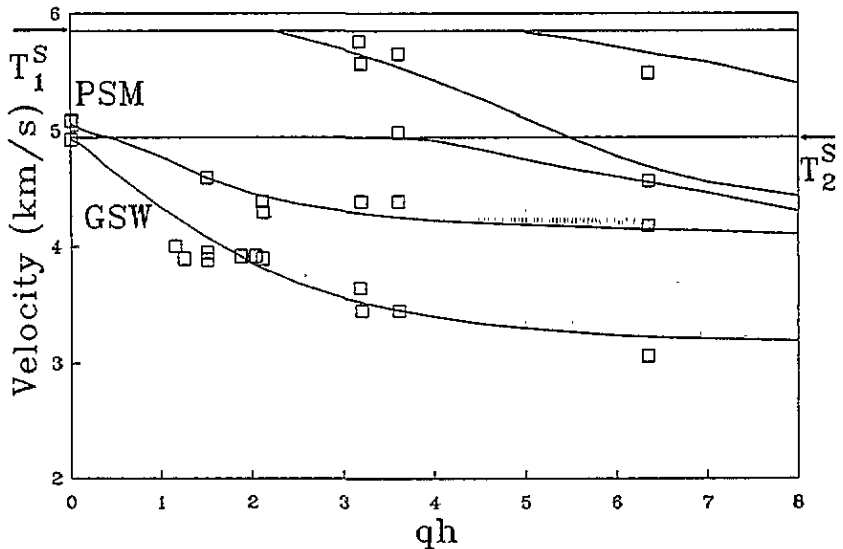


Figure 4. Velocities of the normal surface modes of $\text{CaF}_2/\text{Si}(001)$ structures, for the $\theta = 30^\circ$ propagation direction, as a function of the normalized thickness qh . All the modes have mixed character, and they are represented by full curves. GSW and PSM denote the two lower modes coming from the contributions of the GSW and PSM branches of the substrate material, as explained in the text.

Both GSW and PSM branches of the substrate material contribute significantly to the normal mode spectral content generating the two lower modes. The displacement of GSW keeps its dominantly sagittal orientation for all qh . This is not the case for all other normal modes of the structure. The competition between the properties of the materials of the substrate and layer, which take place as the thickness increases, influences not only the behaviour of their normal-mode velocity values, but also that of their displacement character. Starting with the PSM at $qh = 0$ as a mainly sagittal surface excitation, it transforms into a normal mode and crosses the mainly shear horizontal T_2^S bulk limit line at $qh \sim 0.5$. With further increase in qh this mode gradually changes its character from mainly sagittal to shear horizontal for $qh > 5.0$.

The same transformations, i.e. variation of the displacement character with increasing film thickness, are also observed for the GSW mode appearing initially as predominantly sagittal, $qh \sim 2.0$, and becoming mainly shear horizontal at $qh > 6.5$. On the other hand,

the mode appearing at $qh \sim 3.5$ as nearly pure Love changes its dominant polarization to the sagittal one, $qh > 6.0$.

The behaviour of the two latter modes may also be interpreted in terms of anticrossing of the corresponding 'pure polarized' dispersion curves of figure 3 ($\theta = 45^\circ$) having for $\theta = 30^\circ$ mixed displacement character.

Reasonable correlation between measured and calculated velocity values is observed for $\theta = 30^\circ$, similar to that for $\theta = 0^\circ, 45^\circ$, experimental GSW velocities being systematically lower than the theoretical ones in the range $qh = 1-2$.

5. Correlation between the dynamical properties of $\text{CaF}_2/\text{Si}(001)$ systems and its structure

The agreement between measured and calculated normal velocity values observed for $\text{CaF}_2/\text{Si}(001)$ heterostructures with $h = 61-300$ nm confirms their good structural quality in the GHz range. However, noticeable deviation between measured and calculated GSW velocities was observed at $qh \sim 1$, corresponding to the samples having 61 and 80 nm thicknesses.

We explain this deviation by the peculiarities of the growth and the flattening of CaF_2 epitaxial films deposited on Si (001) wafers. When the epitaxial fluoride layers are put on top of Si (001), the CaF_2 film surface consists of pyramids having a dimension of a few tens of nm with {111} facets [10, 11]. The samples of relatively thick films ($h > 100$ nm) are characterized by total coalescence of the growing pyramids. During the flattening procedure of such a film, top and bottom are reversed and smoothness of the surface on the nm scale is achieved. The thinner films ($h < 100$ nm) may have defects between pyramids that are easily evaporated during the smoothing, and local film discontinuities may appear. The latter worsen the elastic properties, lowering the observed velocity.

The influence of the pyramid structured (unflattened) layer on the normal mode propagation, as well as the comparison with a flattened structure, were studied using samples with a film thickness $h = 150$ nm (figure 5).

In figure 5 one can find the reference spectrum of light scattered by the genuine Si(001) surface at $\theta = 45^\circ$ (a), and those corresponding to the flattened (b), and unflattened (c) samples, the observation conditions being equal. The corresponding calculated surface excitation power spectra are presented in the lower parts of the figure.

One sees that following figure 3 the presence of the $h = 150$ nm film (figures 5(b) and 5(c)) produces the same lowering of the GSW velocity and the appearance of some new normal modes of the structure.

It is clear that the structure of the layer has no detectable influence on the velocities of the sagittal modes. This means that the presence of hillocks and the limiting facets do not perturb strongly the elastic properties of the structure in the GHz range. However, one may remark upon the presence of the Love mode for the unflattened sample, which is not detected in the case of the flattened one.

The absence of this satellite in the spectrum of light scattered by the flattened sample proves that the contribution of the elasto-optic coupling corresponding to the Love mode is negligible. The observation of this mode in the case of the unflattened sample is due to the presence of the shear vertical component of these surface excitations, which is absent for the modes of true Love type. It presumably happens because of the specific structure of the layer with pyramid-like constituent blocks. The pyramids may play a role similar to that of the grooves in a grating discussed in [21]. For the grating, the purely shear horizontal mode

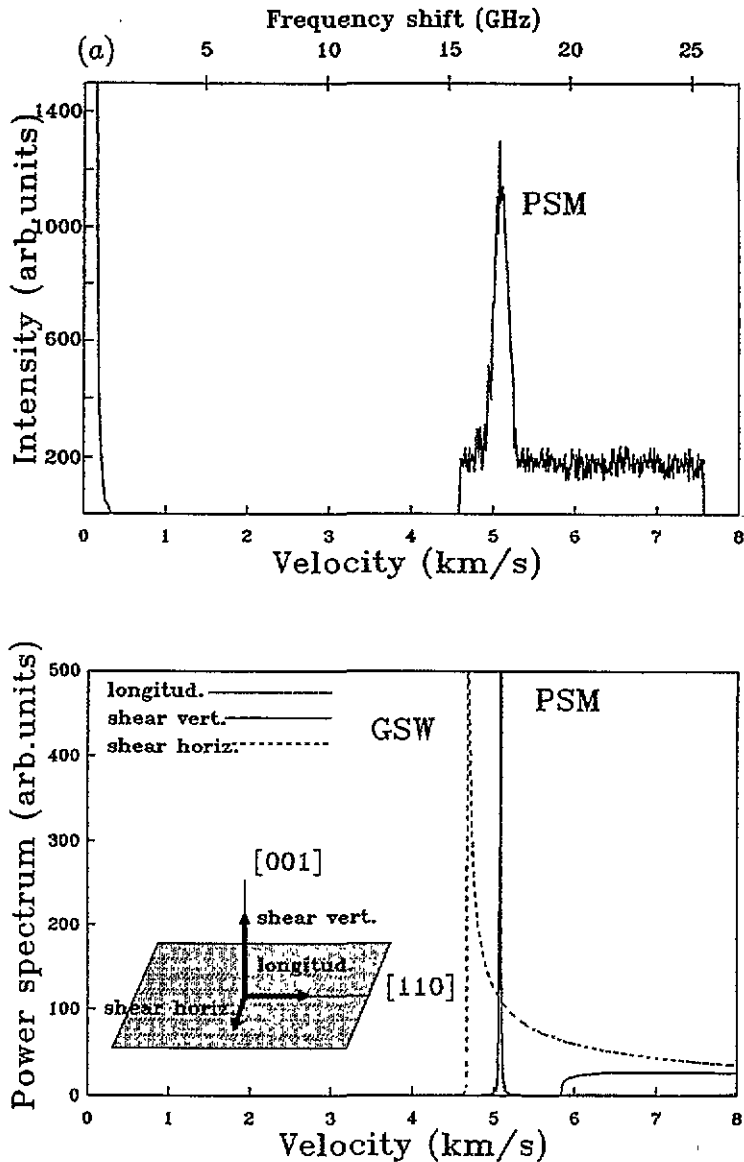


Figure 5. (a) Reference spectrum scattered by the Si (001) surface for $\theta = 45^\circ$, $\alpha = 60^\circ$. The lower part of the figure represents the calculated power spectrum of surface excitations. The character of the different components contributing to these excitations is described in the insert.

propagating along the grooves is transformed into surface excitations, having a non-zero shear vertical component. Following this scheme the Love mode 'breaks' its pure shear horizontal polarization at the surface of the pyramids and a corresponding Brillouin satellite is detected.

The observation of the Brillouin peak corresponding to the Love mode in the unflattened

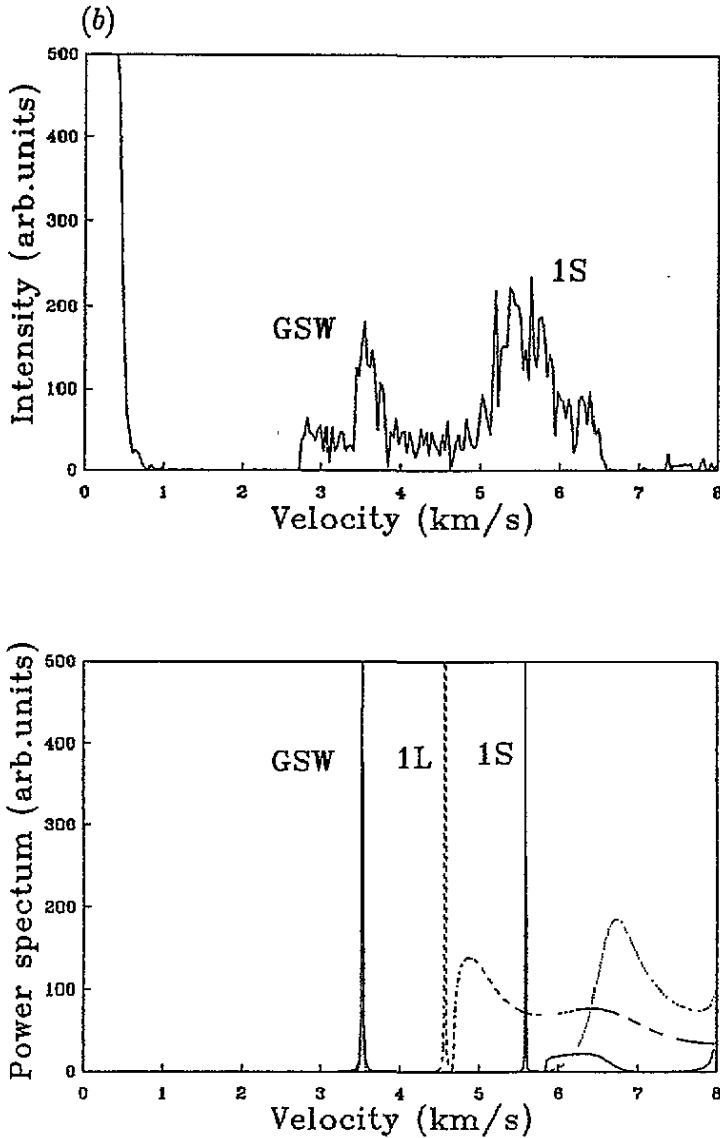


Figure 5. Continued. (b) Spectrum scattered by the flattened sample with $h = 150$ nm.

$h = 150$ nm specimen may also be explained by the lowering of the effective symmetry of the layer because of its macroscopic pyramid-like structure. The lowering of the symmetry for $\theta = 45^\circ$ propagation direction gives a three partial-wave solution instead of the former pure Love mode, and a corresponding Brillouin satellite is detected due to the ripple scattering mechanism.

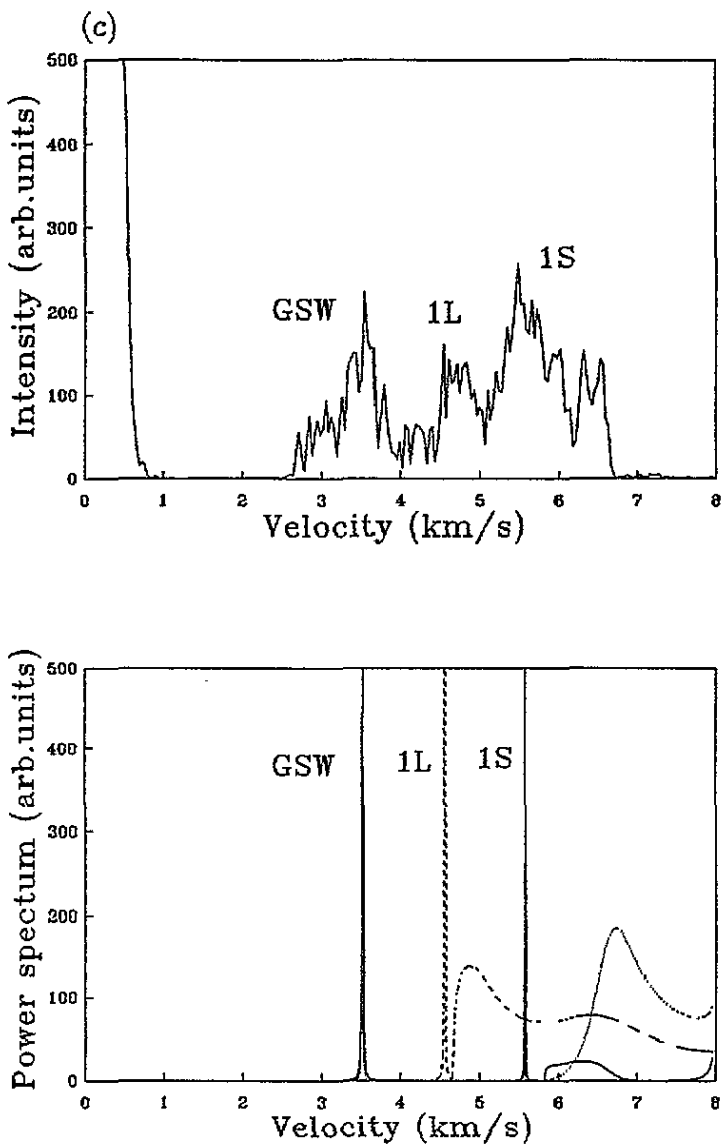


Figure 5. Continued. (c) Same as in (b) for the unflattened sample. The observation of the 1L is explained in the text.

6. Conclusion

The dynamical properties of epitaxial $\text{CaF}_2/\text{Si}(001)$ systems have been studied by using Brillouin spectroscopy. The polarization character of the different modes was analysed as a function of the thickness of the sample, and of the propagation direction. We observed that experimental and calculated velocity values, obtained from a simple elastic continuum

model, in general match each other quite well. Nevertheless, a noticeable deviation between measured and calculated GSW velocities was observed for samples with $h = 61, 80$ nm. This led us to find a correlation between the dynamical properties of $\text{CaF}_2/\text{Si}(001)$ systems and their structure, which is associated with the existence of local film discontinuities produced during the smoothing process. This affects the elastic properties and lowers the velocities.

The influence of the flattened (unflattened) layer on the normal mode propagation was studied with samples having $h = 150$ nm. One may conclude from this study that the structure of the layer has no detectable influence on the velocities of the normal modes, but that it modifies the displacement pattern of the modes.

Acknowledgments

The authors are grateful to Professors F García-Moliner, A M Diakonov and N S Sokolov for helpful discussions. The contribution of VVA and VRV was partially supported by NATO under Collaborative Research Grant 930164.

References

- [1] Farnell G W and Adler E L 1972 *Physical Acoustics* vol IX, ed W P Mason and R N Thurston (New York: Academic) p 35
- [2] Aleksandrov V V, Bottani C E, Caglioti G, Ghislotti G, Marinoni C, Mutti P, Yakovlev N L and Sokolov N S 1994 *J. Phys.: Condens. Matter* **6** 1947
Aleksandrov V V, Saphonov M V, Velasco V R, Yakovlev N L and Martynenko L Ph 1994 *J. Phys.: Condens. Matter* **6** 3347
- [3] Harrison T R, Mankiewich P M and Dayem A H 1982 *Appl. Phys. Lett.* **41** 1102
- [4] Farnell G W 1970 *Physical Acoustics* vol VI, ed W P Mason and R N Thurston (New York: Academic) p 109
- [5] Karanikas J M, Sooryakumar R and Phillips J M 1989 *J. Appl. Phys.* **65** 3407
- [6] Aleksandrov V V, Potapova Ju B, Diakonov A M, Yakovlev N L and Sokolov N S 1994 *J. Phys.: Condens. Matter* **6** 1213
- [7] Aleksandrov V V, Potapova Ju B, Vorob'ev P A, Diakonov A M and Yakovlev N L 1993 *Fiz. Tverd. Tela* **35** 2436 (Engl. Transl. 1993 *Sov. Phys.—Solid State* **35** 1208)
- [8] Aleksandrov V V, Potapova Ju B, Diakonov A M and Yakovlev N L, 1994 *Thin Solid Films* **237** 25
Aleksandrov V V, Diakonov A M, Potapova Ju B and Sokolov N S 1992 *Pis. Zh. Tekh. Fiz.* **18** 44 (Engl. Transl. 1992 *Sov. Tech. Phys. Lett.* **18** 628)
- [9] Gastev S V, Novikov S N, Sokolov N S and Yakovlev N L 1987 *Pis. Zh. Tekh. Fiz.* **13** 961 (Engl. Transl. 1987 *Sov. Tech. Phys. Lett.* **13** 401)
- [10] Fathauer R W and Schowalter L G 1984 *Appl. Phys. Lett.* **45** 519
- [11] Asano T, Ishiwara H and Furukawa S 1988 *Japan. J. Appl. Phys.* **27** 1193
- [12] Holmes D A 1967 *Appl. Opt.* **6** 168
- [13] Nizzoli F and Sandercock J R 1990 *Dynamical Properties of Solids* vol 6, ed H K Horton and A A Maradudin (Amsterdam: North-Holland) p 281.
- [14] García-Moliner F and Velasco V R 1992 *Theory of Single and Multiple Interfaces* (Singapore: World Scientific)
- [15] Aleksandrov V V, Velichkina T S, Potapova Ju B and Yakovlev I A 1992 *Phys. Lett.* **171A** 103
- [16] Aleksandrov V V, Potapova Ju B, Velichkina T S and Yakovlev I A 1993 *Ultrasonics Int.'93, Vienna* (Oxford: Butterworth-Heinemann) p 266
- [17] Barnett D M, Lothe J, Nishioka K and Asaro R J 1973 *J. Phys. F: Met. Phys.* **3** 1083
- [18] Loudon R and Sandercock J R 1980 *J. Phys. C: Solid State Phys.* **13** 2609
- [19] Bortolani V, Marvin A M, Nizzoli F and Santoro G 1983 *J. Phys. C: Solid State Phys.* **16** 1757
- [20] Bortolani V, Nizzoli F, Santoro G and Sandercock J R 1982 *Phys. Rev. B* **25** 3442
- [21] Mayer A P, Zierau W and Maradudin A A 1991 *J. Appl. Phys.* **69** 1942